

Conference Paper

Designing an Eddy Current Brake for Engine Testing

Alexandre José Rosa Nunes and Francisco Miguel Ribeiro Proença Brojo

University of Beira Interior

Abstract

An Eddy Current Brake (ECB) has several advantages making it suitable for using in a dynamometer for testing engines. In this paper, a model is presented which considers the electromagnet's core saturation to predict the performance of an ECB. A design is then proposed for a dual coil, single rotor ECB that meets the design requirement to dissipate a power of 30 kW at 3000 rpm. A comparison between the results obtained for a few different materials considered to be used in the rotating disc are also presented.

Keywords: Antimagnetic force, Dynamometer, Eddy current brake, MATLAB Model

Corresponding Author:

Alexandre José Rosa Nunes
 alexandre.nunes@ubi.pt

Received: 26 November 2019

Accepted: 13 May 2020

Published: 2 June 2020

Publishing services provided by
Knowledge E

© Alexandre José Rosa Nunes and Francisco Miguel Ribeiro Proença Brojo. This article is distributed under the terms of the [Creative Commons Attribution License](#), which permits unrestricted use and redistribution provided that the original author and source are credited.

Selection and Peer-review under the responsibility of the ICEUBI2019 Conference Committee.

1. Introduction

When developing a motor, it is necessary to test and characterize its performance for optimization and suitable rating and application. This can be done with a dynamometer by measuring and then drawing the torque and power output curves as well as its efficiency.

A dynamometer is a device which absorbs the energy of the motor and measures the force produced therefore allowing to measure its torque and power output when the rotational speed is measured as well. In 1905, Morris presented several different methods to absorb this energy and measure such parameters. [1] Among these, the eddy current brake (ECB) presented itself as a promising device to use as a dynamometer.

Wouterse [2] described an ECB, also known as electric retarder, as a machine which dissipates all the mechanically absorbed power as heat in the (thin) disk. It works on the principle that an eddy current is induced around the pole shoe of the coil core when the magnetic flux goes through a rotating conductive disk. The interaction between the magnetic induction and induced currents produce a retarding torque which can, therefore, be used as a brake for determining the torque-speed curves of a motor. This

OPEN ACCESS

method of loading is particularly suitable for testing small motors with a high-speed range since the entire retarding power is converted into heat. [2–4]

The ECB is widely used in several applications such as making high speed trains levitate, setting the different levels of resistance in an exercising bicycle, in dynamometers for automotive testing and in industrial braking systems. [5]

The advantages of the ECB are: [1–7]

1. Simple and robust;
2. Compact size;
3. Less prone to malfunction as there are no moving parts except for the rotating disk;
4. Lack of wear due to no contact between moving components;
5. Noiseless;
6. Lower maintenance costs;
7. Very fast response time;
8. Easy to control;
9. Better performance for both low and high speeds;
10. Uniformity of load after final temperature conditions are reached;
11. Heat produced is not conducted to bearing.

However, it also has some disadvantages such as the braking torque depending on the magnitude of the magnetic field and the velocity of motion. The first can be controlled by varying the electric current that passes through the electromagnet and is limited by the coil core saturation whereas the second is directly proportional to the braking torque available, i.e., the higher the velocity, the higher the braking torque. [5] If the velocity is zero, then so is the braking torque which means it cannot be used for immobilization.

A typical ECB, in its most basic configuration (Figure 1), consists of an electric conductive disk rotating through a magnetic field which induces eddy currents and produces a braking torque. The eddy currents induce a magnetic field which opposes the original magnetic field B .

Three distinct domains can be observed on an ECB at different speeds (Figure 2): [3, 8, 9]

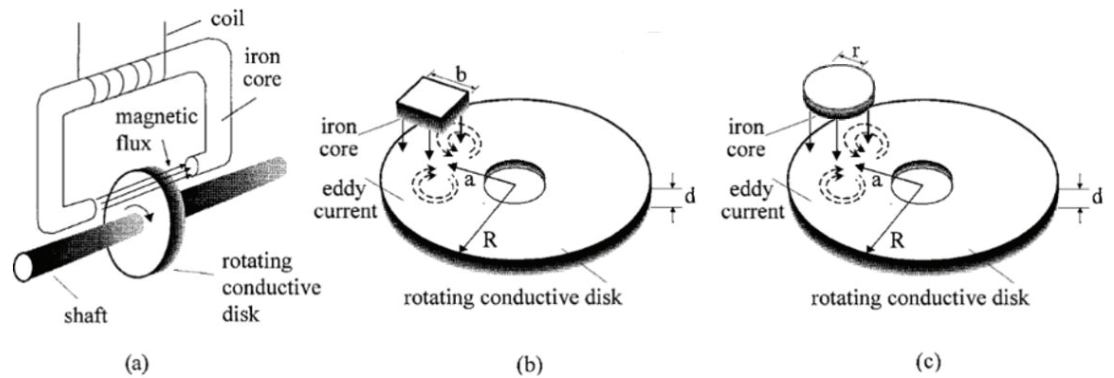


Figure 1: (a) Configuration of an ECB system; (b) and (c) Cross section of the iron core and disk. [6]

1. *Low-speed domain.* At these speeds, the magnetic field induced by the eddy currents is minimal compared to the original magnetic field thus, the magnetic induction B in the air gap is slightly lower than the one at zero speed B_0 . The braking torque and rotating speed are proportional although this correlation diminishes as the speed increases;
2. *Critical-speed domain.* In this region, the magnetic field induced by the eddy currents can no longer be disregarded when compared to B_0 with the magnetic induction B in the air gap being considerably less than B_0 . The braking torque peaks at its maximum value and the corresponding speed is taken as the demagnetization or critical speed;
3. *High-speed domain.* At these speeds, the braking torque becomes inversely proportional to the rotating speed and shows an asymptotical behavior. In fact, for infinite speed, the induced eddy currents will completely cancel the original magnetic field B .

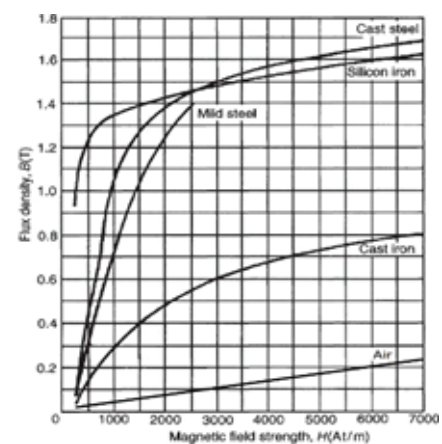
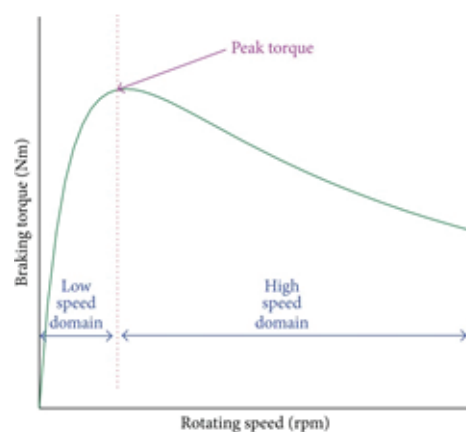


Figure 2: Torque-speed relation on an ECB [3] (left) and B-H curves for four materials (adapted from [10]) (right).

The magnetic field can be produced by either permanent magnets or electromagnets. Although permanent magnets don't need any power to produce a magnetic field, its intensity cannot be controlled. Conversely, electromagnets can quickly change the magnetic field produced by varying the electric current supplied to the coil.

By adding a demagnetized ferromagnetic material to the core of the electromagnet, the external magnetic field H produced by the coil will magnetize this material therefore greatly increasing the magnetic flux density B produced by the electromagnet. However, there is a limit depending on the material properties after which increasing the magnetic field strength won't magnetize the core any further and thus the magnetic flux density will increase linearly, behaving like an air core. In this case, it is said that the core is saturated.

Figure 2 also shows the correlation between the magnetic field strength and magnetic flux density for four materials often used as ferromagnetic cores and an air core.

1.1. Analytical models for predicting eddy brake performance

Over the years many approaches were taken in trying to develop analytical methods to predict the eddy currents in a moving conductor, most of which focused on the low-speed domain.

In 1906, Rudenberg [11] successfully pioneered the study of eddy currents by designing a brake energized by direct current with a cylindrical machine as its base. His theory considered the poles were placed close to each other so sinusoidal functions were accurate enough to describe both the magnetic fields and current patterns.

Following Rudenberg's work, Smythe [12] presented a paper in 1942 where the distribution of the eddy currents induced in a rotating conductive disk around the pole were studied. In his work, Smythe started by modelling the ECB by implying a magnetic potential theory and then deriving the Maxwell's equations to describe the demagnetization effects. His work was accurate for the low-speed domain but inaccurate for the high-speed domain.

Continuing Smythe's work, in 1974 Schieber [13] presented a paper with the same results as Smythe but extended the theory to consider the case of a linearly moving strip, although no work was done regarding the high-speed domain.

In 1991, Wouterse [2] followed the works presented by Smythe and Schieber to validate the results previously obtained for the low-speed domain as well as attempt to model the eddy currents induced in the high-speed domain.

Later in 1995, Simeu and George [8] were the first to apply the magnetic circle theory in order to model an ECB. This model calculated the amount of eddy currents and braking torque by assuming that all the power dissipated by the eddy currents generated braking torque. However, this model did not account for the eddy current demagnetization and thus was only suitable for describing the behavior of an ECB in the low-speed domain.

In 1999, Lee [6] presented work where an ECB and its controller were developed to be used as an alternative to conventional hydraulic brake systems. An approximate theoretical model was presented to perform a braking torque analysis, which was then modified based on experimental results.

Recently, Zhou et al [3] presented in 2015 a paper in which a mathematical model based on the magnetic circle theory was developed for an ECB design while introducing the concept of antimagnetic force. Additionally, simulations based on the model developed were carried out to predict the braking torque characteristics and investigate the factors that influenced torque generation by variations of the parameters in the ECB's structures design. This model showed promising results in predicting the performance for the low and high-speed domains since it accounted for the influence of both the demagnetization and temperature effects on the braking torque attenuation.

2. Mathematical Model

The following mathematical model was developed based on the work of Zhou et al. [3]

2.1. Magnetic Circle Theory

The Ampere-Maxwell equation relates the electric currents and magnetic flux as

$$\oint_l H dl = N.I \quad (1)$$

where l is the equivalent length of the magnetic circle, H is the magnetic field strength, N is the number of turns of the coil and I is the current applied to it. In a single electromagnet composed of one core and coil, the path of integration is a closed circle and so $\oint_l H dl = H.l$. The magnetic flux Φ can be calculated by

$$\Phi = B.A = \frac{\mu.N.I.A}{l} \quad (2)$$

where B can be calculated by $B = \mu.H$ and represents the magnetic flux density, A is the crosssection area of the pole shoe and μ is the magnetic permeability. The basic magnetic theory is then described by

$$\Phi = \frac{\mathfrak{F}}{\mathfrak{R}} \tag{3}$$

with $\mathfrak{F} = N.I$ and $\mathfrak{R} = l/(\mu.A)$ being defined as the magnetic force and reluctance, respectively. The combined magnetic force \mathfrak{F} is the sum of the magnetic and antimagnetic forces and the overall reluctance \mathfrak{R} is the overall resistance in electric circles.

2.2. Derivation of the ECB Model

Before deriving the ECB model, its configuration must be considered. In this paper, a single rotating disk with two opposed C-shaped electromagnets (Figure 3) producing the magnetic field were considered for its ease of manufacturing, simple maintenance and easier balancing and performance prediction. However, the ECB was modelled as a single coil-core system (Figure 1) based on its equivalent magnetic circle (Figure 4).

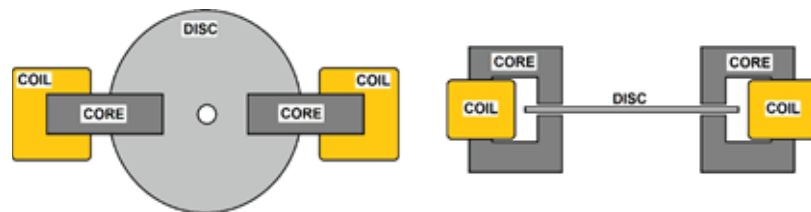


Figure 3: Illustration of the ECB considered in this paper.

The following assumptions were made for deriving the ECB mathematical model:

1. The cross-section area of the magnetic flux in the rotating disk is equal to the cross- section area of the pole shoe;
2. The distance from the center of the pole shoe to the rotating center of the disk is significantly higher than the disk thickness ($a \gg d$), therefore the reluctance in axial direction $\mathfrak{R}_{d_{ax}}^*$ is also significantly lower than in radial direction $\mathfrak{R}_{d_{ra}}^*$ and thus the latter can be ignored;
3. The variation of temperature T of the rotating disk over time is not considered;
4. The magnetic flux density does not increase upon reaching saturation.

Taking these assumptions into consideration, the equivalent magnetic circle of the ECB was rebuilt into a simplified equivalent magnetic circle (Figure 4) consisting of a

magnetic circle with magnetic and antimagnetic forces as well as the air-gap, coil and rotating disk magnetic reluctances, connected in series.

The first step was to model the variation of the electric conductivity σ of the rotating disk due to the increase in temperature. The electric conductivity σ can be calculated as

$$\sigma = \frac{1}{\rho_0(1 + \alpha.T)} \tag{4}$$

where ρ_0 is the electric resistivity of the disk at 20°C, α is the temperature coefficient of resistance and T is the temperature of the disk.

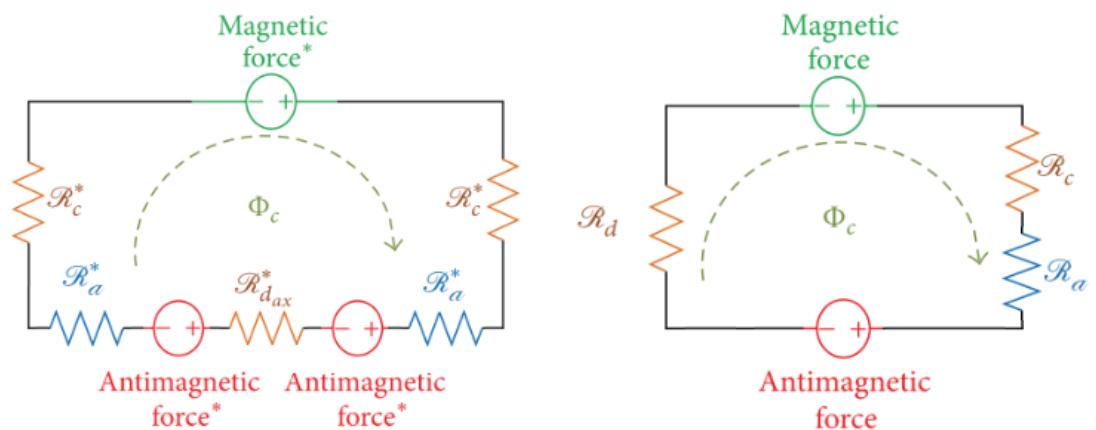


Figure 4: Equivalent Magnetic Circle of the ECB (left) and Simplified Equivalent Magnetic Circle of the ECB with coil, air-gap and disk reluctances (left) (adapted from [3]).

From the Simplified Equivalent Magnetic Circle (Figure 4) and (3), the magnetic flux in one coilcore can be calculated by

$$\Phi_c = \frac{\mathfrak{F}_i - \mathfrak{F}_{eddy}}{\mathfrak{R}_c + \mathfrak{R}_a + \mathfrak{R}_d} \tag{5}$$

where \mathfrak{F}_i is the magnetic force generated by the applied current in the coil and \mathfrak{F}_{eddy} is the defined antimagnetic force produced by the eddy currents induced in the rotating disk. The magnetic reluctances of the coil, air-gap and rotating disk are \mathfrak{R}_c , \mathfrak{R}_a and \mathfrak{R}_d , respectively, and can be calculated as

$$\mathfrak{R}_c = \frac{l_c}{\mu_c \cdot \mu_0 \cdot A} \tag{6}$$

$$\mathfrak{R}_a = \frac{l_g - d}{\mu_0 \cdot A} \tag{7}$$

$$\mathfrak{R}_d = \frac{d}{\mu_r \cdot \mu_0 \cdot A} \tag{8}$$

where l_c is the length of equivalent magnetic circle in the core, μ_c is the relative permeability of the core, l_g is the distance between the pole shoes, d is the thickness

of the rotating disk, μ_0 is the permeability of vacuum and μ_r is the relative permeability of the rotating disk.

The reluctance outside the core \mathfrak{R}_g can be defined as

$$\mathfrak{R}_g = \mathfrak{R}_c + \mathfrak{R}_a + \mathfrak{R}_d \quad (9)$$

Since the relative permeability of a ferromagnetic core μ_c is several times higher than that of the vacuum, with a value of 5000 for iron [14], the reluctance of the core \mathfrak{R}_c is minimal. It can then be ignored and thus $\mathfrak{R}_g = \mathfrak{R}_a + \mathfrak{R}_d$. Equation (5) can now be rewritten as

$$\Phi_c = \frac{\mathfrak{F}_i - \mathfrak{F}_{eddy}}{\mathfrak{R}_g} \quad (10)$$

The magnetic force \mathfrak{F}_i can be calculated as

$$\mathfrak{F}_i = N.I \quad (11)$$

where N is the number of turns of the coil and I is the current applied to it. Also, based on Figure 1, the antimagnetic force \mathfrak{F}_{eddy} generated by the eddy currents induced in the rotating disk can be calculated by

$$\mathfrak{F}_{eddy} = \oint_s J_e dS = J_e . d . r \quad (12)$$

where d is the thickness of the rotating disk, r is the radius of the core's cross-section and J_e is the current density of the eddy currents induced at the center of the pole. These can be calculated by

$$J_e = \sigma . a . (\omega \times B_c) \quad (13)$$

In (13), a is the distance from the rotating center to the center of the pole shoe area, ω is the angular speed of the rotating disk and B_c is the magnetic flux density in one coil-core which can be calculated by

$$B_c = \frac{\Phi_c}{A} \quad (14)$$

Considering (12) and (13), the antimagnetic force \mathfrak{F}_{eddy} can be calculated as

$$\mathfrak{F}_{eddy} = \sigma . a . d . r \left(\omega \times \frac{\Phi_c}{A} \right) \quad (15)$$

From (5), \mathfrak{F}_{eddy} can also be calculated as

$$\mathfrak{F}_{eddy} = N . I . - \Phi_c . \mathfrak{R}_g \quad (16)$$

Hence, from (15) and (16), Φ_c can be calculated as

$$\Phi_c = \frac{N . I}{\mathfrak{R}_g + \sigma . a . d . r . \omega / A} \quad (17)$$

As seen before, the magnetic flux density in one coil-core was taken as $B_c = \Phi_c/A$. However, the saturation of the ferromagnetic core was not considered. This was included by having $B_c \leq B_{sat}$, with B_{sat} being the limit of magnetic saturation of the core. Therefore, when the core is not saturated, (13) can be rewritten as

$$J_e = \sigma.a.(\omega \times B_c) = \sigma.a. \left(\omega \times \frac{\Phi_c}{A} \right) \quad (18)$$

Otherwise, (13) can be rewritten as

$$J_e = \sigma.a.(\omega \times B_{sat}) \quad (19)$$

The total power dissipated by the eddy currents induced by one coil-core can be calculated by integrating $\rho.J_e^2$ over the cylindrical volume $V_{cyl} = A.d$. The power dissipated P_d is then

$$P_d = \rho.J_e^2.V_{cyl} = \rho.J_e^2.A.d \quad (20)$$

The braking torque T_b can simply be calculated by

$$T_b = \frac{P_d}{\omega} \quad (21)$$

The critical speed ω_c for which the torque is maximum can be calculated by

$$\omega_c = \frac{l_g - d}{\mu_0.\sigma.a.d.r} + \frac{d}{\mu_r.\mu_0.\sigma.a.d.r} \quad (22)$$

A nonferromagnetic disk has a relative permeability close to that of vacuum, therefore (22) can be simplified to

$$\omega_c = \frac{l_g}{\mu_0.\sigma.a.d.r} \quad (23)$$

From the power dissipated and the braking torque of each coil-core, the total power dissipated and braking torque of the ECB can be calculated by multiplying P_d and T_b of each coil-core by the number of coils n_{coil} .

2.3. Design requirements for the ECB

The ECB designed in this paper is intended to be applied to a dynamometer in an engine test stand. Consequently, the following design considerations were taken:

1. The material for the rotating disk was chosen to be nonferromagnetic to prevent torsion stresses on the disk;
2. It was decided to use an iron core with a saturation limit of around 2T. [5, 6, 9] However, a saturation limit of 1.5T was considered to account for any material impurities, manufacturing errors or further losses in the core;

3. To prevent coil saturation for the engine's entire operating domain it was decided that the core should not be saturated at angular speeds over 750 rpm since most small engines have idle speeds over this value;
4. It was considered a square shape for the iron core. Compared to a round pole shape, a rectangular pole shape increases the maximum brake torque while keeping the critical speed nearly unchanged. Furthermore, the total power dissipation at low and critical speeds is greater for rectangular than for round pole shapes. [14]
5. The main design requirement was a power dissipation of 20kW at 3000rpm due to the performance of the engine intended to be tested. It is advised to increase the power dissipation by 35-40 per cent to allow for hysteresis losses and higher harmonics.[4] Consequently, a 50 per cent increase was considered for a power dissipation of 30 kW at 3000rpm as a requirement for designing the ECB.

2.4. MATLAB Development

The model previously presented was implemented in MATLAB according to the flowchart presented in Figure 5. An iterative process was then followed to find a suitable design that met the design requirements.

The resulting model parameters are defined in Table 1, where b is the side dimension of the square pole shoe, n_{coil} is the number of coils considered in the simulation and T is the temperature of the rotating disk. The temperature of the rotating disk was assumed to be 200°C since a forced-air convection cooling system is intended to be installed. In Table 2, the properties of the materials considered for the rotating disk in the simulation are presented. [15–18] The three ferromagnetic materials are for comparison only since the material intended to be used is nonferromagnetic.

3. Simulation Results

A maximum angular speed ω_{max} of 6000 rpm was taken as a typical value for an engine at load. After the iterative process the torque, power dissipated and magnetic field flux density curves were obtained and presented in Figure 6.

The maximum torque obtained for the nonferromagnetic materials was 96.41 N.m at a critical speed of 123 rpm for Copper, 99.41 N.m at a critical speed of 188 rpm for Aluminum and 97.51 N.m at a critical speed of 3369 rpm for Stainless Steel. For

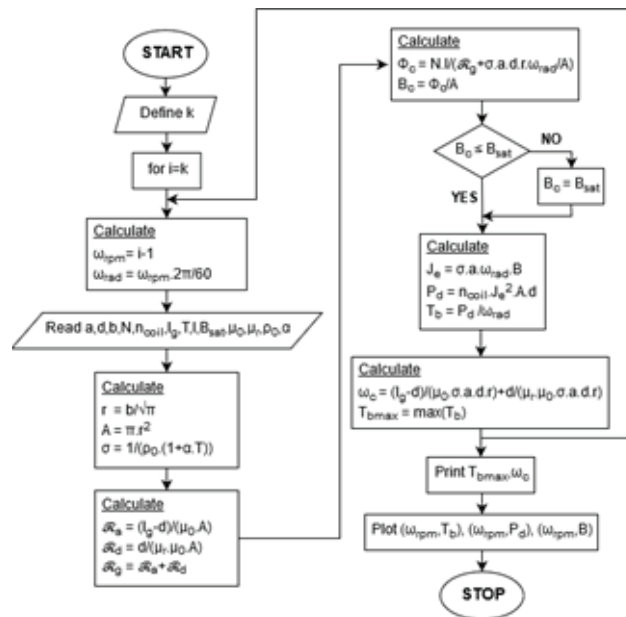


Figure 5: MATLAB Flowchart.

TABLE 1: Parameters for the ECB Model

Parameter	Value	Unit
A	150	mm
d	4	mm
b	40	mm
r	22,57	mm
A	1600	mm ²
ω_{max}	6000	rpm
N	3350	-
n_{coil}	2	-
l_g	7	mm
μ_0	$4\pi \times 10^{-7}$	H/m
T	200	°C
I	3	A
B_{sat}	1,5	T

the ferromagnetic materials it was 206.35 N.m, 206.30 N.m and 206.37 N.m at critical speeds, respectively, of 590 rpm for Iron, 681 rpm for Mild Steel and 2512 rpm for Electrical Steel.

At the design required angular speed of 3000 rpm, the power dissipated calculated was 4.60 kW, 6.74 kW and 30.53 kW for Copper, Aluminum and Stainless Steel, respectively. As for Iron, Mild Steel and Electrical Steel the results were a power dissipation of 25.03 kW, 28.04 kW and 61.17 kW, respectively. Additionally, at the maximum angular speed of 6000 rpm, a power dissipation of 4.79 kW, 7.15 kW, 56.43 kW, 27.68 kW, 31.46

TABLE 2: Properties of the Materials for the Rotating Disk

Material	Parameter	Value	Unit
Copper	ρ_0	$1,69 \times 10^{-8}$	Ω/m
	α	$4,30 \times 10^{-3}$	$^{\circ}C^{-1}$
	μ_r	1	-
Aluminium	ρ_0	$2,65 \times 10^{-8}$	Ω/m
	α	$4,50 \times 10^{-3}$	$^{\circ}C^{-1}$
	μ_r	1	-
Austenitic Stainless Steel	ρ_0	$73,00 \times 10^{-8}$	Ω/m
	α	$0,94 \times 10^{-3}$	$^{\circ}C^{-1}$
	μ_r	1,02	-
Iron	ρ_0	$9,70 \times 10^{-8}$	Ω/m
	α	$5,00 \times 10^{-3}$	$^{\circ}C^{-1}$
	μ_r	5000	-
Mild Steel	ρ_0	$14,00 \times 10^{-8}$	Ω/m
	α	$3,00 \times 10^{-3}$	$^{\circ}C^{-1}$
	μ_r	2000	-
Electrical Steel	ρ_0	$59,00 \times 10^{-8}$	Ω/m
	α	$2,00 \times 10^{-3}$	$^{\circ}C^{-1}$
	μ_r	7000	-

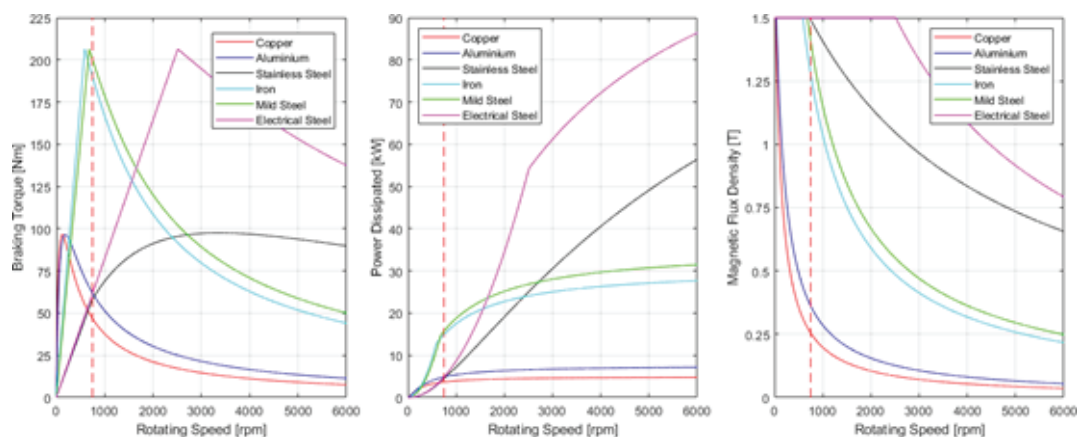


Figure 6: Graphical representation of Braking Torque vs Rotating Speed.

kW and 86.36 kW were estimated for Copper, Aluminium, Stainless Steel, Iron, Mild Steel and Electrical Steel, correspondingly. Finally, the core is no longer saturated at angular speeds of 26 rpm for Copper, 39 rpm for Aluminium and 730 rpm for Stainless Steel, 590 rpm for Iron, 682 rpm for Mild Steel and 2513 rpm for Electrical Steel.

4. Conclusions

This paper presents a MATLAB model that predicts the performance on both low and high-speed domains of an ECB to be applied to an engine dynamometer. This model is useful as a simple tool for predicting the performance of an ECB in a preliminary design process.

Following the work of Zhou et al [3], the model developed introduces the electro-magnet core saturation and its impact on the performance, as well as the influence of using several different materials for the rotating disk. The first is of utmost importance to account for the limitation introduced by the material used as the core of the electro-magnet, while the latter is relevant to the speed domain intended to be optimized.

From the results, one can conclude that due to the high speeds achieved by the rotating disk, a material with higher electrical resistivity is more adequate since it will increase the critical speed.

As far as ferromagnetic materials are concerned, only Electrical Steel was able to perform consistently better than Stainless Steel due to its high resistivity and permeability. However, the coil core remains saturated until an angular speed of 2513 rpm.

Acknowledgments

This work has been supported by the project Centro-01-0145-FEDER-000017 – EmaDeS – Energy, Materials and Sustainable Development, co-financed by the Portugal 2020 Program (PT 2020), within the Regional Operational Program of the Center (CENTRO 2020) and the European Union through the European Regional Development Fund (ERDF). The authors wish to thank the opportunity and financial support that permitted to carry on this project and C-MAST/ Centre for Mechanical and Aerospace Science and Technologies.

References

- [1] D. K. Morris and G. A. Lister, “The eddy current brake for testing motors”, in *Journal of the Institution of Electrical Engineers*, vol. 35, no. 175, pp. 445-468, September 1905
- [2] J. H. Wouterse, “Critical torque and speed of eddy current brake with widely separated soft iron poles”, in *IEE Proceedings B – Electric Power Applications*, vol. 138, no. 4, pp. 153-158, July 1991

- [3] Q. Zhou, X. Guo, G. Tan, X. Shen, Y. Ye and Z. Wang, "Parameter Analysis on Torque Stabilization for the Eddy Current Brake: A Developed Model, Simulation, and Sensitive Analysis", in *Mathematical Problems in Engineering*, 2015
- [4] D. Gonen and S. Stricker, "Analysis of an Eddy-Current Brake", in *IEEE Transactions on Power Apparatus and Systems*, vol. 84, no. 5, pp. 357-361, May 1995
- [5] D. J. T. Cruz, "Design of an Innovative Car Braking System using Eddy Currents", Master Thesis, University of Victoria, 2005
- [6] K. Lee and K. Park, "Optimal robust control of a contactless brake system using an eddy current", in *Mechatronics* 9, pp. 615-631, 1999
- [7] S. Sharif, J. Faiz and K. Sharif, "Performance analysis of a cylindrical eddy current brake", in *IET Electric Power Applications*, vol. 6, no. 9, pp. 661-668, November 2012
- [8] E. Simeu and D. Georges, "Modeling and control of eddy current brake", in *IFAC Proceedings Volumes*, vol. 28, no. 8, pp. 109-114, July 1995
- [9] G. Sokolov, "Analysis of electrodynamic brake for utilization in systems with rotating shafts", Thesis, Saimaa University of Applied Sciences, 2016
- [10] J. Bird, "Electrical Circuit Theory and Technology, Fifth Edition, Bell & Bain Ltd, Glasgow, Great Britain, 2014.
- [11] R. Rüdtenberg, "Energie der Wirbelströme in elektrischen Bremsen und Dynamomaschinen", Enke, 1906
- [12] W. R. Smythe, "On eddy currents in a rotating disk", in *Electrical Engineering*, vol. 61, no. 9, pp. 681-684, September 1942
- [13] D. Schieber, "Braking torque on rotating sheet in stationary magnetic field", in *Proceedings of the Institution of Electrical Engineers*, vol. 121, no. 2, pp. 117-122, February 1974
- [14] M. O. Gulbahce, D. A. Kocabas and F. Nayman, "Investigation of the effect of pole shape on braking torque for a low power eddy current brake by finite elements method," *2013 8th International Conference on Electrical and Electronics Engineering (ELECO)*, Bursa, 2013, pp. 263-267
- [15] <http://www.nessengr.com/technical-data/resistivity/> (Accessed on 20/03/2019)
- [16] J. D. Kraus and K. R. Carver, "Electromagnetics", International Student Edition, 2nd Edition, McGraw-Hill, 1981
- [17] C. Moosbrugger, "ASM Ready Reference: Electrical and Magnetic Properties of Metals", ASM International, 2000
- [18] J. R. Barnes, "Robust Electronic Design Reference Book", Volume 2: Appendices, Springer US, 2004